Cell. Mol. Life Sci. (2016) 73:4531–4545
DOI 10.1007/s00018-016-2233-y

Cellular and Molecular Life Sciences

ORIGINAL ARTICLE

The growth determinants and transport properties of tunneling nanotube networks between B lymphocytes

Anikó Osteikoetxea-Molnár[1] · Edina Szabó-Meleg[2,3] · Eszter Angéla Tóth[1] · Ádám Oszvald[1] · Emese Izsépi[1] · Mariann Kremlitzka[1] · Beáta Biri[4] · László Nyitray[4] · Tamás Bozó[5] · Péter Németh[6] · Miklós Kellermayer[5,7] · Miklós Nyitrai[2,3] · Janos Matko[1]

Received: 17 December 2015 / Revised: 13 April 2016 / Accepted: 19 April 2016 / Published online: 28 April 2016

Abstract Tunneling nanotubes (TNTs) are long intercellular connecting structures providing a special transport route between two neighboring cells. To date TNTs have been reported in different cell types including immune cells such as T-, NK, dendritic cells, or macrophages. Here we report that mature, but not immature, B cells spontaneously form extensive TNT networks under conditions resembling the physiological environment. Live-cell fluorescence, structured illumination, and atomic force microscopic imaging provide new insights into the structure and dynamics of B cell TNTs. Importantly, the selective interaction of cell surface integrins with fibronectin or laminin extracellular matrix proteins proved to be essential for initiating TNT growth in B cells. These TNTs display diversity in length and thickness and contain not only F-actin, but their majority also contain microtubules, which were found, however, not essential for TNT formation. Furthermore, we demonstrate that Ca^{2+}-dependent cortical actin dynamics exert a fundamental control over TNT growth-retraction equilibrium, suggesting that actin filaments form the TNT skeleton. Non-muscle myosin 2 motor activity was shown to provide a negative control limiting the uncontrolled outgrowth of membranous protrusions. Moreover, we also show that spontaneous growth of TNTs is either reduced or increased by B cell receptor- or LPS-mediated activation signals, respectively, thus supporting the critical role of cytoplasmic Ca^{2+} in regulation of TNT formation. Finally, we observed transport of various GM_1/GM_3^+ vesicles, lysosomes, and mitochondria inside TNTs, as well as intercellular exchange of MHC-II and B7-2 (CD86) molecules which may represent novel pathways of intercellular communication and immunoregulation.

Keywords Membrane nanotubes · Intercellular matter transport · Trogocytosis · Membrane protrusion · Superresolution microscopy · Fluorescence imaging

Electronic supplementary material The online version of this article (doi:10.1007/s00018-016-2233-y) contains supplementary material, which is available to authorized users.

✉ Janos Matko
janos.matko@ttk.elte.hu

1 Department of Immunology, Eötvös Loránd University, Budapest, Hungary

2 Department of Biophysics, Medical Faculty, University of Pécs, Pecs, Hungary

3 MTA-PTE Nuclear-Mitochondrial Interactions Research Group, Pecs, Hungary

4 Department of Biochemistry, Eötvös Loránd University, Budapest, Hungary

5 Department of Biophysics and Radiation Biology, Semmelweis University, Budapest, Hungary

6 Environmental Chemistry Research Group, Research Centre for Natural Sciences, Budapest, Hungary

7 MTA-SE Molecular Biophysics Research Group, Budapest, Hungary

Introduction

Membrane nanotubes or tunneling nanotubes (TNTs), first described a decade ago, are thin, long cellular protrusions interconnecting cells [1, 2]. Since then many interesting functional features were reported and proposed for them, such as intercellular signal transfer and transport of membrane or viral proteins, prions, vesicles, nucleic acids, or even organelles [3–5]. Surfing of bacteria or prions along TNTs [6–8], long distance intercellular transport of ions

[9], quantum dots [10], and electrical coupling through TNTs between developing neurons were also reported [11, 12]. These nanotubular connections gained most attention so far in cells of the nervous and immune systems, including neurons, astrocytes, activated microglia, T-, B-, and NK cells, macrophages, and their targets. As recently reviewed, TNTs can also grow between many other cell types, such as human (HEK) or rat (NRK) kidney cells and mesothelial cells [13–15], and show a high diversity in their morphology and structure [15].

Interestingly, cellular infection by vaccinia or herpes virus may by itself induce formation of long membrane protrusions connecting adjacent cells, which can be assisted by p21-activated kinase (PAK) activity [16]. HIV-1 virus was also reported to exploit membrane nanotubes between T cells for spreading, but growing TNTs between T cells was not influenced by the virus infection itself [3]. Due to technical (primarily optical) limitations, only a few „quasi in vivo-imaging" data are available that demonstrate long, nonlinear TNTs between antigen-presenting dendritic cells (DCs) in rat corneal membranes [17, 18]. TNT-like structures were also observed in chick [19], quail, zebrafish [20], and mouse embryos [21], suggesting that TNTs may also play a role in coordination of cell migration and differentiation. However, explicit demonstration of functional TNTs within the tissue environment would be essential for understanding their physiological functions.

TNTs have been investigated in simplified experimental model systems such as liposomes and proteoliposomes and also by theoretical approaches that set the foundation for biological studies [22–27]. Similarly to other membranous nanostructures such as extracellular vesicles or exosomes [28–30], TNTs gained special attention in immunology and neuroscience because they can also mediate the intercellular exchange of matter (protein, lipid, DNA and miRNA molecules or even organelles) via 'trogocytosis'. Thus, it is anticipated that TNTs may open novel regulatory pathways for some critical immune cell effector functions such as T cell activation, cytokine or antibody production, phagocytosis or cell killing [15, 31, 32]. Moreover, as quantum dots or other molecules could be transported through nanotubular connections between cardiac myoblast cells [10], TNTs may be a therapeutic target for nanobead-conjugated drug delivery.

Despite the continuously accumulating knowledge about membrane nanotubes, several fundamental questions about the molecular and genetic mechanisms controlling their growth as well as their in vivo functional significance remained open. In the immune system, antibody-producing B lymphocytes are key cellular components of the adaptive humoral immune response where TNTs may play important roles. However, in contrast to T lymphocytes and macrophages [31, 32], TNTs between B cells are still largely unexplored and poorly characterized [2, 33, 34].

In the present work, we explored several basic control mechanisms of nanotube growth, such as the key extra- or intracellular factors determining the growth-retraction equilibrium of B cells TNTs. These processes as well as the transport properties of TNTs were monitored using Live Cell Confocal Laser Scanning Microscopy (LC-CLSM), Total Internal Reflection Microscopy (TIRF), and Structured Illumination Microscopy (SIM) at superresolution. Our results show that mature primary murine and human B cells, or B cell lines, but not immature ones, can spontaneously form extended nanotubular connection networks under physiological conditions and that their growth can be differentially modulated by various cellular stimuli (by antigen, LPS, etc.).

Our observations highlight the importance of the integrin-fibronectin/laminin interaction and of cell spreading in initiating TNT growth. By investigating the role of actin or microtubular networks in TNT growth, we demonstrate here that Ca^{2+}-dependent actin-filament dynamics exert a fundamental control on growth-retraction equilibrium of nanotubes. The data also provide new insight into TNT growth control by non-muscle myosin 2 motor proteins. Finally, with respect to the intercellular transport mechanisms along TNTs, time lapse supperresolution microscopy revealed a bidirectional transport of membranous vesicular structures between interconnected B cells. In addition, antigen-presenting MHC molecules or immune costimulatory B7 family proteins can also travel between two adjacent B cells in the membrane of the long nanotubes. Such intercellular exchange may be a novel pathway for the regulation of antigen presentation or T cell activation in lymphoid organs.

Materials and methods

Cells, cell staining, cell-treatments

A20 mature (ATCC TIB208), mCherry-actin expressing A20 [35], X16C immature marginal zone (ATCC TIB-209), 38C13 immature [36] murine B cells, and JY human B lymphoblastoid (ATCC 7744) cell lines were cultured in RPMI-1640 medium (Sigma-Aldrich, St. Louis, MO, USA). 2PK3 mature murine B cells (ATCC TIB-203) was cultured in Dulbecco's modified Eagle's medium (Sigma Aldrich). All cell lines were supplemented with L-glutamine, Na-pyruvate, 2-mercaptoethanol (except in the case of JY human cell line), $NaHCO_3$, penicillin, nonessential amino acids, vitamins, and 10 % FCS, at 37 °C, and 5 % CO_2. Mouse splenic lymphocytes and human tonsillar B lymphocytes were used promptly

following isolation and purification. All the treatments of animals (mice) in this research followed the guidelines of the Institutional Animal Care and Ethics Committee at Eötvös Loránd University that operated in accordance with permissions 22.1/828/003/2007 issued by the Central Agricultural Office, Hungary. Human B cells from tonsils of children aged 2–8 were used with ethical permission of ethical committee of S. Laszlo-S. Istvan Hospital Budapest (25/EB/2013). Informed consent was obtained according to the Declaration of Helsinki.

For imaging nanotube growth, cells were labeled with Alexa647- or Alexa488-conjugated cholera toxin B subunit (CTX-B) $GM_{1/3}$-ganglioside-specific probes (40 μg/ml) (Life Technologies, Carlsbad, USA) on ice for 10 min or alternatively with DiO (5 μM), DiI (5 μM) or DiD (5 μM) (Life Technologies) dyes for 5 min at 37 °C. Anti-α5 (10 μg/ml), anti- α6 (5 μg/ml) (eBioscience, San Diego, USA), anti-β1 (5 μg/ml) (BioLegend, San Diego, USA) or anti- β4 (AbD Serotec, Langford Lane, Kidlington, UK) monoclonal antibodies were used to label the two integrin chains on B cells (20 min, ice).

MHC-II and B7 molecules were labeled with anti-MHC-II (ATCC TIB-120™ M5/114) or anti-CD86 [37] antibodies for 10 min, 37 °C. To colocalize MHC-II and GM1 gangliosides in nanotubes, cells were incubated after MHC-II labeling and with Alexa647-CTX-B for further 10 min. Lysosomes and mitochondria were labeled with MitoTracker (50 nM) and LysoTracker (75 nM) (Thermo Fisher Scientific, Waltham, MA USA) for 30 min, 37 °C, then cells were washed once.

B cells were stimulated with LPS polyclonal activator (10 μg/ml) (Sigma-Aldrich) for 18 h at 37 °C in CO_2 incubator or with anti-IgG $F(ab')_2$ (10 μg/ml) (Jackson ImmunoResearch, Suffolk, UK) for 20 min, at identical conditions. The cytoplasmic Ca^{2+} level of the cells was adjusted with ionomycin ionophore (Sigma-Aldrich) or thapsigargin, an inhibitor of the endoplasmic reticulum Ca^{2+}-ATPase (Sigma-Aldrich), prior to or following a 1-h TNT-growth period. EGTA (Sigma-Aldrich) (4 mM) was added to the culture medium before ionomycin addition to test for the specificity of its effects. To inspect the viability of the cells after treatment with ionomycin, cells were incubated in Annexin-binding buffer with 5 μl FITC-Annexin V (BioLegend) (for detection of phosphatidylserine translocation, an early apoptosis marker) for 10 min at RT, and 10 μg/ml PI (Sigma-Aldrich) (for detection of membrane permeabilization as late apoptosis marker) for 5 min. These samples were then measured by Becton–Dickinson FACS Aria III flow cytometer.

To stain actin, cells were fixed with 4 % paraformaldehyde (PFA) for 10 min, then permeabilized with 0.1 % Triton X-100 + 1 % BSA (Sigma-Aldrich) for 20 min, and incubated with Alexa 488-phalloidin (Life Technologies) for 45 min. All of these steps were carried out at room temperature (RT). Microtubules were stained, in identical steps, with anti-tubulin antibody (Abcam, Cambridge, UK) for 1 h at RT, then washed, and labeled with secondary antibody (goat anti-rat Northern light493; R&D Sytems, Minneapolis, MN, USA). Actin polymerization was inhibited by incubating the cells with latrunculin B (5–50 μM) (Sigma-Aldrich) for 20 min or with cytochalasin D (20–100 μM) (Sigma-Aldrich) for 2 h at 37 °C, 5 % CO_2.

To inhibit microtubule assembly/disassembly cells were incubated with P3456 paclitaxel (Taxol) (1–10 μM) (Life Technologies) and nocodazole (1–30 μM) (kind gift from Dr. Judit Ovádi, Institute of Enzymology, Hungarian Academy of Science, Hungary) for 20 min at 37 °C, 5 % CO_2. To investigate myosin 2A, cells were fixed and permeabilized as described above and labeled with anti-myosin 2A (BioLegend) primary Ab + FITC-conjugated secondary Ab. In functional assays of non-muscle myosin 2A for nanotube growth, para-nitro-blebbistatin (10–50 μM) (kind gift from Dr. András Málnási-Csizmadia, Department of Biochemistry, Eötvös University, Hungary), a specific inhibitor of myosin 2 activity and Y-27632 (10–40 μM) (Sigma-Aldrich), a specific inhibitor of Rho kinase activity were used.

Methods

Analysis of TNT growth

To investigate the effect of substrate surface on TNT growth, cells were cultured either on untreated borosilicate surface, or on a borosilicate surface pre-coated with 0.1 mg/ml poly-L-Lysine coat (Sigma-Aldrich), or 0.3 mg/ml collagen (Sigma-Aldrich, Type I solution from rat tail) or 10 μg/ml fibronectin (RT, overnight, Sigma Aldrich) or 10 μg/ml laminin proteins (RT, 2 h, Sigma-Aldrich) in microplate wells (Ibidi Planegg/Martinsried) at physiological conditions (37 ± 0.1 °C; CO_2: 5 %). Typically a cell density of 3×10^5 cells/cm^2 and an incubation time of 1 h were used for imaging. Images were taken with IX81 inverted Laser Scanning Confocal Microscope (Olympus, Hamburg, Germany), using 60× oil immersion objective (N.A.: 1.1).

High-resolution imaging

For superresolution imaging of B cells and their nanotubes, Structured Illumination Microscope (SIM), set up on a Zeiss Elyra S_1 (63×; N.A.: 1.4 objective) microscope was used. Images were acquired with five grid rotations. Atomic force microscopic (AFM) images were collected

with an MFP3D instrument (Asylum Research, Santa Barbara, CA, USA) with B cells incubated on fibronectin coats for 2 h at 37 °C in 5 % CO_2 atmosphere and fixed with 4 % PFA (15 min, RT). Samples were subsequently washed with distilled water and dehydrated with 20, 40, 60, 96 % and absolute ethanol. Non-contact-mode images were recorded in air with a 0.8–1 Hz line-scanning rate using a silicon cantilever (OMCL AC 160TS, Olympus, Japan) oscillated at its resonance frequency (300–320 kHz, typically).

For scanning electron microscopic (SEM) imaging (ZEISS EVO 40XVP) B cells were incubated on fibronectin coats for 2 h, then fixed, and dehydrated [38].

TIRF microscopic images of TNTs were collected using a YAG laser (532 nm, 50 mW CW, JDS Uniphase, Milpitas, CA, USA) for excitation, and a TIRF objective (100×, 1.49 NA, Olympus, Japan) and an EMCCD camera (iXonEM + 885, Andor Technology, UK) for image acquisition. TIRF images were acquired using the Andor Solis program and post-processed with ImageJ [39].

Statistical analysis

Frequency of TNT forming cells was calculated from at least 500 cells/sample and given as mean percentage ± SD. It is defined as the ratio of cells growing at least one nanotube to the total cell number in the field. Branching frequency was defined as the ratio of nanotube branching sites to the total number of nanotube-forming cells in the field. Cell spreading evaluation [35] and the analysis were made using ImageJ software (Wayne Rasband, NIH, Bethesda, MD, USA, using plugins available at website: Wright Cell Imaging Facility, Toronto, ON, Canada) and SigmaPlot 10.0 statistics software.

Flow cytometric measurements were carried out on a BD FACSAria III cytometer (Becton–Dickinson, Franklin Lakes, NJ, USA) using DIVA software (BD Biosciences, San Jose, CA, USA).

Results

Formation of membrane nanotube network between B cells is highly controlled by their microenvironment

First we explored what conditions are optimal for B cells to form extensive nanotubular connections. Mature murine A20 B cell line and human tonsil primary B cells (Fig. 1a–c) as well as murine splenic or other mature murine and human B cell lines (2PK3, JY; not shown) were found to spontaneously grow various types of membrane nanotubes and even complex networks after 1 h on fibronectin coats at 37 °C, in a 5 % CO_2 atmosphere. These representative images were recorded by live cell (LC-CLSM) imaging of a 1:1 mixture of B cells stained with DiD (green) and DiI (red) cell tracking dyes. B cells of mature phenotype spontaneously form uni- or bidirectionally growing TNTs (Fig. 1a, middle and right, respectively), while immature (38C13) B cells show neither significant spreading nor TNT growth (Fig. 1a, left). Similarly to T cells [40], B cells are often interconnected by TNTs following a cell division as marked by the presence of a midbody; moreover, they can also be connected by multiple (thin and thick) TNTs or can form even three way junctions (Fig. 1b).

Representative high-resolution AFM and SEM images of B cell nanotubes (Fig. 1c) show a typical TNT morphology [3] in most cases. Interestingly, extremely long (occasionally >150 μm) and thin TNTs were also observed between B cells from human tonsils (Fig. 1c) under identical conditions.

Formation of nanotubes between B lymphocytes were observed only under live-cell imaging conditions (37 °C; 5 % CO_2 atmosphere) and on fibronectin (or laminin) coats, but not on other coating materials, such as poly-L-lysine or collagen, or in the absence of coating materials (Fig. 1d). TNT formation reaches saturation in 1–2 h under the above conditions at an optimal initial cell density of 3×10^5 cells/cm^2. At a lower density such as 0.5–2 $\times$ 10^5 cells/cm^2 the frequency of TNT-forming cells decreased to 1–3 %, while at higher density such as 0.9–1.5 $\times$ 10^6 cells/cm^2 TNT formation was still detectable although the number of cells was too high to be accurately counted. The length and width of B cell TNTs proved to be heterogeneous with means of 22 μm and 650 nm, respectively, as assessed by SIM superresolution imaging (Fig. 1e). Their average length is comparable with that of T cell TNTs while their average thickness is markedly larger [40]. Together, the above findings indicate that nanotube growth strongly depends on membrane fluidity, as shown by the temperature dependence, the density of cultured cells, and the properties of the substrate surface.

Because the substrate surface appeared to be a key factor in TNT growth, we further analyzed it in greater detail. Cell surface integrins are known to selectively interact with fibronectin through the flexible FBN III domain or with other matrix proteins [41]. Thus, we first investigated whether the expression level of the α5/β1 integrin, dominant in A20 B cells, correlates with the observation that these cells frequently form TNTs while immature 38C13 cells do not (Fig. 1a). While 38C13 cell line expresses neither α5, nor β1 integrin chains at detectable levels (Fig. 2a), mature A20 cells show high expression of both chains (Fig. 2b). Similarly, a low α5/β1 integrin expression was accompanied by a lack of TNT

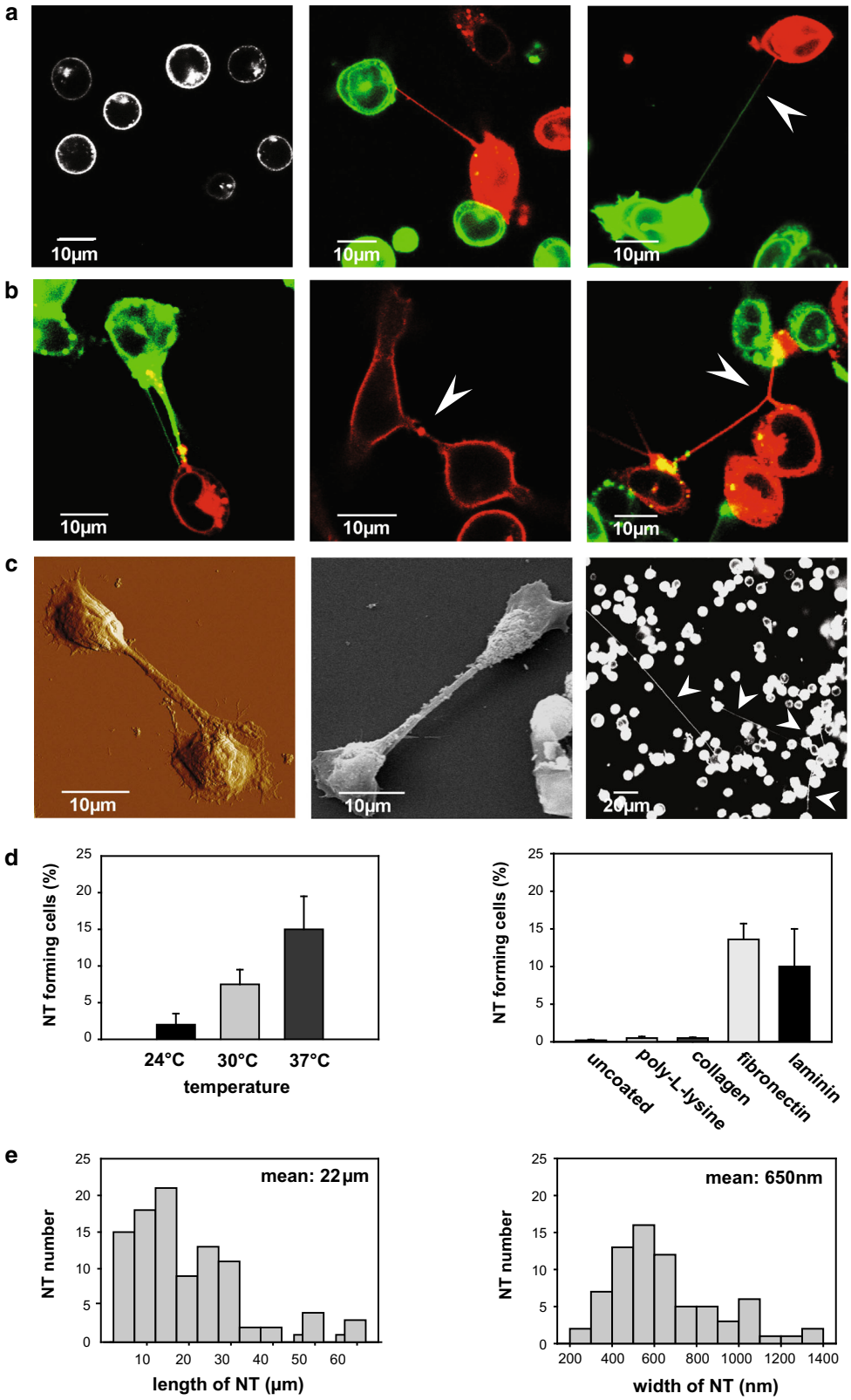

Fig. 1 Mature, but not immature, mouse and human B cells spontaneously form nanotubular connections under physiological conditions. **a** Representative live cell confocal images of immature 38C13 (*left*; monochrome DiO fluorescence) or mature A20 (*middle and right*) murine B cells stained with 1:1 mixtures of DiO (*green*) and DiI (*red*) dyes and incubated for 1 h. Tunneling nanotubes (TNTs) can grow unidirectionally (**a**, *middle*) or bidirectionally (**a**, *right*: *dual color*; *see white arrow*). **b** A20 B cells are often connected with multiple (*thin and thick*) TNTs (*left*), can form TNTs following cell division (*middle*; see midbody, *white arrow*), or can form even three way junction (*right*; *see white arrow*). **c** High-resolution AFM (*left*) and SEM (*middle*) images of A20 B cells show TNT morphology. Extremely long (≥100 μm) and thin TNTs can be detected in the culture of freshly isolated human tonsil B cells (*right*; *see white arrows*). **d** B cell TNTs form optimally at 37 °C (*left*) and on fibronectin or laminin coats (*right*). **e** B cell nanotubes are largely diverse in both their length (*left*) and width (*right*) with means (±SD) of 22 ± 10 μm and 650 ± 250 nm, respectively. Mean and SD values for TNT forming cell % were derived from at least five independent experiments, from ca. 500 cells/sample

formation in X16C marginal zone B cells (data not shown). Simultaneous addition to the A20 B cell culture of monoclonal antibodies against both the α5 and β1 polypeptide chains of the integrins significantly blocked both the extent of cell spreading and TNT-formation while the addition of either antibody alone did not (Fig. 2c). In addition to

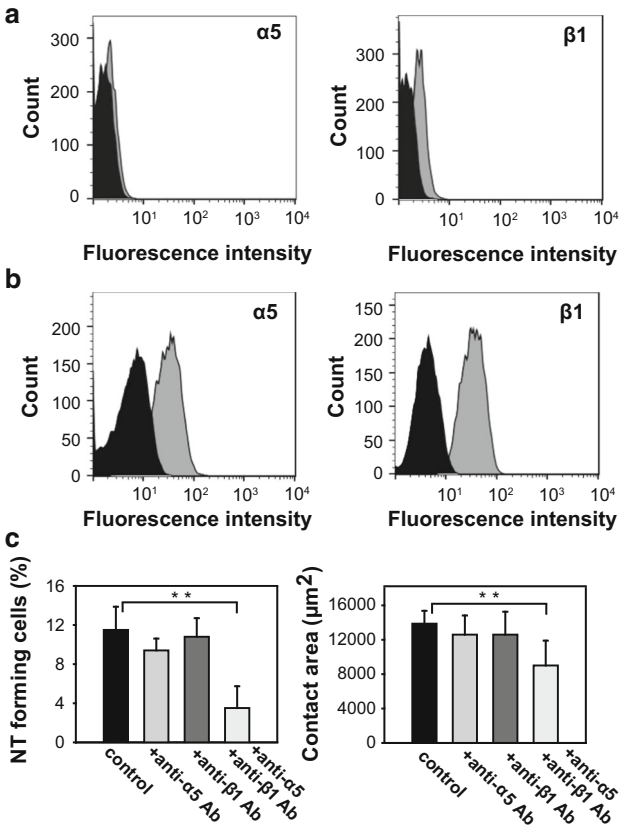

Fig. 2 **a** Flow cytometric histograms show lack of α_5 (*black* isotype control antibody; *grey* anti-α_5 antibody) (*left*) or β_1 (*black* isotype control antibody; *grey* anti-β_1 antibody) (*right*) integrin chains on 38C13 immature murine B cells. **b** Both integrin chains were detected on mature A20 murine B cells, α_5 (*black* isotype control antibody; *grey* anti-α_5 antibody) (*left*) and β_1 (*black* isotype control antibody; *grey* anti-β_1 antibody) (*right*). **c** In A20 B cells NT growth frequency (*left*) and cell adhesion/spreading (*right*) were found to be dependent on the interaction between fibronectin and both of its integrin receptor subunits ($\alpha_5\beta_1$), as evidenced by the lack of significant changes in these properties upon individual blocking of each integrin subunit but significant reduction upon simultaneous blockade of both subunits (*left and right*) (**$p \leq 0.01$)

fibronectin, we also investigated whether laminin could also be a key adhesion factor in TNT formation. However, instead of the α5/β1 integrin receptor for fibronectin, as potential receptors for laminin, α6/β4 and α6/β1 integrins were proposed [42]. Therefore, we investigated and found that the A20 B cells also express α6, but not β4 integrin chain, while positive for β1chain. Furthermore, we also found that A20 B cells failed to adhere to the laminin surface, and, therefore, did not form TNTs, when we simultaneously applied blocking antibodies against both α6 and β1 integrin chains. Antibodies against the α6 and β1 integrin chains, applied alone, blocked or strongly decreased the TNT formation (Supplementary Fig. 1). Together, these findings suggest that a direct contact of the cell surface with its microenvironment via selective integrin–ligand interactions [43, 44] is a critical factor in its commitment towards TNT formation and may also explain the differences in the TNT-forming capacity of immature and mature B cells.

B cell nanotubes are capable of intercellular transport of immunoregulatory molecules in their membrane and vesicles inside the tube

In cholera toxin-labeled B cells cultured for 1 h we discovered, using SIM, large vesicles within the cell body and the nanotubes (Fig. 3a). Considering that cholera toxin is a good marker of exosomes and other extracellular vesicles [45] they may be multivesicular bodies which are known to be involved in formation and secretion of exosomes and other microvesicles. Following the labeling of B cell plasma membranes with Alexa488-CTX-B, appearance in high-resolution fluorescence images of membrane-covered fluorescent vesicles within the cytoplasm and TNTs of B cells suggests that these structures originate from plasma membrane lipid bilayers. Note that no significant difference was found in the TNT frequency if the cells were labeled with indocarbocyanine derivatives (DiO, DiD or DiI) or with fluorescent cholera toxin B subunit (data not shown). Time-lapse SIM video-imaging showed a bidirectional intercellular traffic of these vesicular structures between adjacent B cells (Supplementary Movie S1, S2), indicating that most of the thick TNTs were open-ended. The tracks show a very slow motion of vesicles between the adjacent B cells, compared to that reported, e.g. for quantum dots in cardiac myoblasts [10]; therefore, further detailed analysis is required to reveal the mechanism including the possible motor proteins responsible for this transport.

The membrane of the TNTs is also abundant in MHC-II proteins (Fig. 3b, d, e) and CD86 immune costimulatory molecules (Fig. 3c, f, g), as shown by staining with fluorescent antibodies of the nanotubes bridging A20 murine B cells (and also 2PK3 cells; data not shown). These TNT membrane regions are also enriched in gangliosides (Fig. 3b) as revealed by staining with fluorescent CTX-B. The possibility that MHC-II or immune costimulatory proteins can be exchanged between B cells through nanotubes, via membrane- or vesicular transport, is suggested by the presence of the labeled MHC-II or CD86 molecules in the cell membrane at the opposite side of the TNT, close to the TNT connection point as well as in other membrane regions of the neighbor cell (Fig. 3d, e, f, g). Furthermore, we found both lysosomes (Fig. 3h) and mitochondria (Fig. 3i) inside the TNTs; therefore, the B cell TNTs may also mediate intercellular transport of these organelles. Furthermore, we examined the frequency of these elements in the TNTs and found that 52 % of the TNTs contain MHC-II protein, 50 % contained CD86 molecules, while 11 % showed lysosomes, and 32 % showed mitochondria.

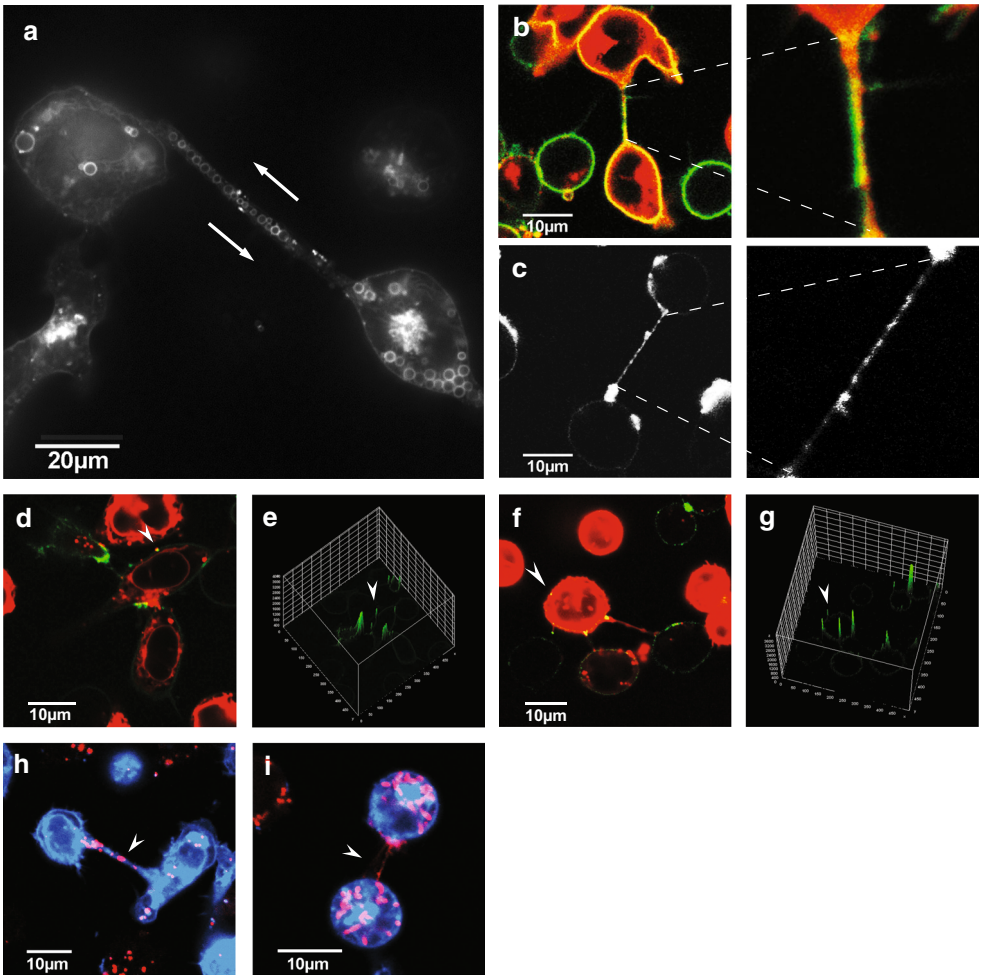

Fig. 3 B cell nanotubes may mediate bidirectional transport of membrane vesicles inside the tubes and also transport of molecules essential for T cell activation in the membrane of TNTs. **a** Representative superresolution (SIM; lateral resolution: 80–90 nm) image of TNTs connecting adjacent A20 B cells. The fluorescence on these images originates from extracellular labeling of cell membrane gangliosides with Alexa488-cholera toxin B (CTX-B) before a 1 h incubation for TNT formation at live cell imaging conditions (37 °C, 5 % CO_2). The image clearly shows existence of large and small vesicles in the cell bodies and the latter ones along the TNTs. (The average diameter of vesicles is 1.6 μm) (The intercellular transport of vesicles across TNTs and its bidirectional feature is also demonstrated by Supplementary Movies S1, S2.) **b** Representative confocal image of TNT-connected A20 B cells shows abundance of MHC-II/peptide complexes (*green*) along the TNTs (*left*), in a highly colocalized fashion with GM1/3 gangliosides (*red*), markers of lipid rafts (zoom: *right*). **c** B7-family costimulatory proteins (CD86) are also enriched along the TNTs (*left*), in a clustered fashion (zoom: *right*). CLSM images also demonstrate that both MHC-II/peptide (*green*) (**d**, **e**, *white arrow*) and B7-2/CD86 molecules (*green*) (**f**, **g**, *white arrow*) were able to reach the connected cell through the TNT membrane. Analysis of fluorescence intensity of the 'acceptor' cells shows that both molecules appear in their cell membrane close to the TNT, or even farther from the TNT connection (see *white arrow*). **h**, **i** In addition, lysosomes (Lysotracker, *violet*; **h**) and mitochondria (MitoTracker, *violet*; **i**) were also detected in B cell TNTs, suggesting the possibility of intercellular transport. (Movement of mitochondria within nanotubes is shown on Supplementary Movie S3.) Each representative image was derived from three independent experiments (≥100 TNT) (**$p \leq 0.01$)

(Data from three independent experiments with ≥100 TNTs). In addition, movement of mitochondria within TNTs from one cell to the neighbor was also observed as shown in Supplementary Movie S3.

Nanotube growth of B cells is differentially modulated by various activation stimuli

Spontaneous emergence of nanotubes is a property of resting B cells (Fig. 1a). Therefore, we investigated how various activation stimuli can affect nanotube growth in B cells. Activation of B cells with anti-BCR antibody, leading to antigen receptor-specific stimulation and a rise in cytoplasmic Ca^{2+}, results in a slight, but significant decrease in TNT-growth frequency (Fig. 4c). Interestingly, stimulation of B cells through a Ca^{2+}-independent pathway with LPS (polyclonal activator) causes an opposite effect; the frequency and branching of TNTs increases significantly (Fig. 4b, c). Thus, various stimuli may differentially modulate nanotubular

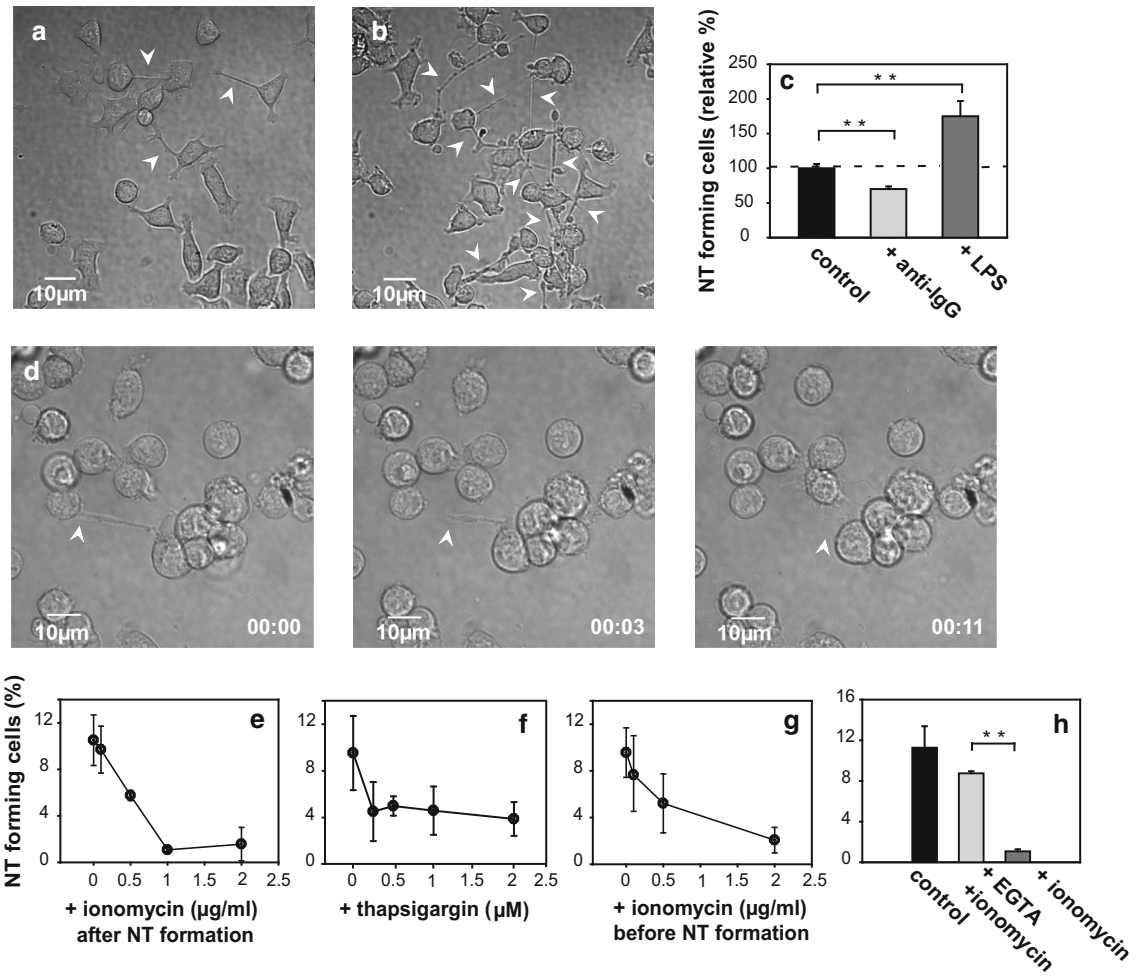

Fig. 4 TNT-growth of B cells is modulated by cellular activation and the cytoplasmic free Ca^{2+} level. **a**, **b** Representative DIC images show increased TNT number (*white arrows*) in LPS-treated (**b**) vs. untreated (**a**) A20 B cells. **c** Monoclonal (BCR-mediated) activation of B cells by anti-Ig antibody (10 μg/ml) slightly decreased, while polyclonal activation with LPS lipopolysaccharide (10 μg/ml) significantly enhanced TNT-formation. **d** Time lapse images (from *left to right*) show that Ca^{2+} influx induced by 1 μg/ml ionomycin Ca^{2+}-ionophore resulted in rapid withdrawal (typically in 10–20 s) of TNT connecting two cells (position of the free end of the NT is shown by *white arrow*). (See also Supplementary Movie S4.) **e**–**g** Ionomycin or thapsigargin (an inhibitor of SER Ca^{2+}-ATPase) both inhibited TNT-growth in a concentration-dependent fashion, if applied after TNT-growth reached saturation in the culture (**e**, **f**). Notably, ionomycin could also prevent TNT-growth if applied for 5 min, (and then washed out from the samples) before culturing for 1 h for TNT-growth (**g**). **h** EGTA (4 mM) applied extracellularly almost completely reversed the ionomycin-induced effect. The mean and SD values depicted on the panels were determined from more than three independent experiments (≥500 cells/sample)

connections of B cells, in a Ca^{2+}-dependent or independent fashion.

Dynamics of cytoplasmic free Ca^{2+} and actin filaments exert a key control over the growth-retraction equilibrium of B-cell nanotubes

Recently, we have shown an inverse relationship between the cytoplasmic free Ca^{2+} level and the actin polymerization-depolymerization equilibrium in B cells [35]. A similar, coordinated control of Ca^{2+}-mobilization and cytoskeletal remodeling was reported for T cell activation/synapses as well [46]. Here we also show that ionomycin-induced Ca^{2+}-influx results in a rapid retraction (in 11 s) of a previously connective (ca. 25 μm long) nanotube in a demonstrative time lapse image series (Fig. 4d) (Supplementary Movie S4). Ionomycin effectively reduces the number of TNTs in B cell cultures in a concentration-dependent manner when applied after the TNT numbers reached saturation (Fig. 4e). Thapsigargin, an inhibitor of endoplasmic reticulum Ca^{2+}-ATPase also causes a similar rapid decline of TNT number (Fig. 4f). Notably, in addition to reducing the number of existing TNTs, ionomycin can also prevent the formation of new TNTs in a concentration-dependent manner if applied for 5 min to the cells (and then washed out) before the 1 h culture (Fig. 4g).

Excess of extracellular EGTA (4 mM), which sequesters the available extracellular Ca^{2+}, can almost completely reverse this effect (Fig. 4h). Moreover, ionomycin did not in itself have a cytotoxic effect on the cells as proved by verifying their viability with flow cytometry using Annexin V as a marker of early apoptosis and propidium iodide (PI) as a marker of late apoptosis and necrosis. Compared to the percentage of early and late apoptotic cells in the control ionomycin-free sample, the ratio of early and late apoptotic cells did not show a significant increase in cells treated with ionomycin (Supplementary Fig. 2). These data altogether suggest that Ca^{2+}-dependent remodeling either by recovery or degradation of the cortical actin filament network in B cells is a fundamental mechanism involved in the growth and retraction of nanotubes. Furthermore, treatment with actin polymerization blockers cytochalasin D and latrunculin B induced a concentration-dependent suppressive effect of TNT-growth confirming the essential role of F-actin in nanotube formation (Fig. 5d). Addition of the actin stabilizer jasplakinolide, an inhibitor of dynamic elongation and depolymerization alike, also significantly inhibits TNT-growth further supporting the essential role of F-actin dynamics in nanotube formation (Fig. 5d). As expected from the above evidence, TIRF and SIM images confirmed that most B cell nanotubes contain F-actin (Fig. 5a, b). However, unlike T cells [31, 40], the majority of B cell TNTs also contain microtubules (Fig. 5c).

In contrast to the inhibition of actin filament dynamics, inhibition of microtubule polymerization with nocodazole or of their stabilization with paclitaxel does not affect nanotube formation (Fig. 5e). Moreover, the actin polymerization blocker latrunculin B is still able to induce retraction/collapse of nanotubes even in the presence of the microtubule stabilizer paclitaxel (Fig. 5e). These data suggest that microtubules are not directly involved in the growth-retraction equilibrium of B cell nanotubes. However, they may contribute to other TNT functions such as mediating vesicular transport.

Non-muscle myosin 2 controls TNT growth in B cells

Myosin motor proteins have been implicated in many aspects of nanotubular networks. Among others, they have been reported to mechanically pull nanotubes from liposome models on actin cable supports [23] or to generate force in the filopodia of Dorsal Root Ganglion neurons [47]. In lymphocytes, non-muscle myosin 2A (NM2A) has been implicated in various in vivo or in vitro functions, such as the formation and stability of immunological synapses [48, 49] or transendothelial migration [50]. We found that NM2A is also expressed in all B cells (Fig. 6a). Moreover, it is abundantly localized in the spontaneously formed nanotubes interconnecting the cells (Fig. 6b). Interestingly, efficient blockers of myosin 2 activity, such as p-nitro-blebbistatin [51], largely enhance both the growth and the degree of branching of TNTs (Fig. 6d, e), similarly to Y-27632, an inhibitor of Rho-associated protein kinase (ROCK) that is involved in activating non-muscle myosin 2 (Fig. 6c). The small decline in TNT number at higher (>30 μM) p-nitro-blebbistatin concentrations is presumably due to a cytotoxic effect which is confirmed by the altered morphology of the cells (data not shown). In conclusion, our data clearly show that NM2A has a role in the regulation of nanotube generation and dynamics. Although its exact function is not yet known, it is generally assumed that force generation by NM2A is responsible for the proper regulation of membrane protrusions [52]. Thus it is reasonable to assume that NM2A is directly involved in the regulation/limitation of nanotube growth.

Discussion

The aim of this study was to explore the basic morphological and structural features of nanotubular networks interconnecting B cells. The possible functional relevance of such membrane tethers was another important subject of this study, as well as the major factors and mechanisms controlling growth or retraction of TNTs. We found that under physiological conditions both mouse and human B cell lines or primary B cells of mature phenotype, but not the immature ones, could spontaneously form membrane nanotubes with a characteristic tunneling TNT morphology and structure in 10–15 % of the cells.

The interaction between the cell surface integrins and extracellular matrix components such as fibronectin and laminin was found to be the most important condition in the initiation of nanotube outgrowth. Obermajer et al. [53] have previously reported that cathepsin-X mediated β2-integrin activation in T cells leads to cell polarization and promotes outgrowth of TNTs. Fibronectin and laminin were reported to highly influence cell adhesion and signaling either alone or in concerted action, via interacting with various integrin receptors [54, 55]; moreover, the ECM composition was shown to determine even the complex transcriptional response of human embryonic kidney cells to stimulation of other receptors [56]. In addition, laminins were also shown to modulate development or effector function of B cells through mostly α6-integrins [42, 57]. Thus, it is possible that their selective promoting effect vs. collagen on nanotube growth is also due to their yet unexplored signaling events in lymphocytes.

Others have also reported on the importance of integrin–ligand interactions in cell adhesion, migration, and in

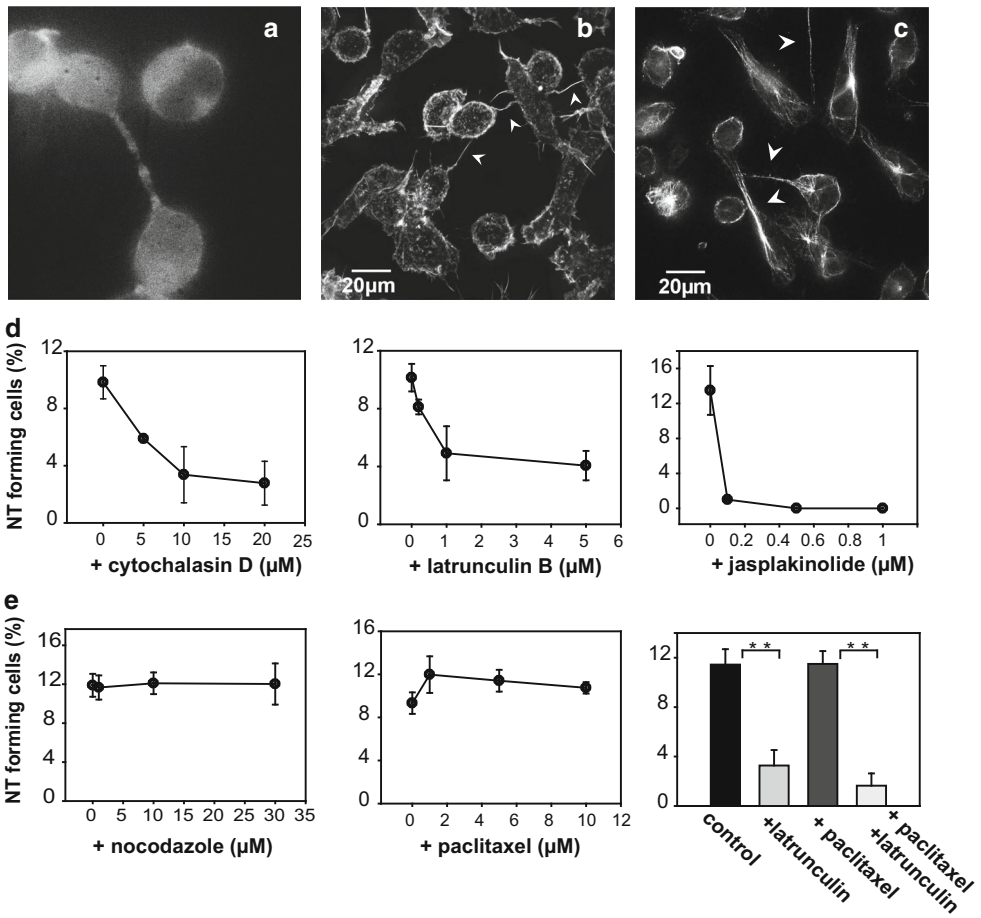

Fig. 5 **a** Representative TIRF image of m-Cherry-actin transfected and **b** SIM image of Alexa488-phalloidin stained A20 B cells demonstrating (by *white arrows*) that the nanotubes always contain actin filaments. **c** Majority of the TNTs also contain microtubules as assessed by SIM images of Alexa488-anti-tubulin stained cells (*white arrows*). **d** Cytochalasin D (*left*) and latrunculin B (*middle*) as inhibitors of F-, and G-actin polymerization, respectively, efficiently blocked nanotube growth such as jasplakinolide (*right*) did, in a concentration dependent manner. **e** In contrast, nocodazole, inhibitor of microtubule polymerization (*left*) or paclitaxel (taxol) a stabilizer of microtubule structure (*middle*) left TNT growth unchanged. Latrunculin B (5 μM) could initiate a ca. fourfold reduction in nanotube number even in the presence of paclitaxel (10 μM) stabilizing microtubules (*right*). The mean TNT-frequencies and the SD values displayed on the panels were calculated from three independent experiments (≥300 cells in each) (**$p \leq 0.01$)

general the rearrangement of cortical cytoskeleton [41, 43, 44]. These data together with our findings highlight the importance of integrin–extracellular matrix interaction and cell adhesion/spreading as key factors in initiating outgrowth of membrane nanotubes connecting lymphocytes. Furthermore, immature B cells that do not express the dominant fibronectin-receptors, $\alpha_5\beta_1$ integrins, showed no sign of adherence, spreading, and TNT outgrowth also supporting the importance of integrin–extracellular matrix interactions in TNT formation.

TNT-growth likely also depends on the actual lipid composition of the plasma membrane, which determines the fluidity, elasticity, bending rigidity, and the local curvature of the membrane which are all important factors in the process [22, 25, 26]. Another key membrane determinant of the stability/growth of nanotubes [27, 58] may be the level of raft gangliosides (GM_1/GM_3), which we have found to be much lower in immature than mature B cells (Tóth EA, 2016, unpublished data), suggesting a role of these raft lipids in the initiation and dynamics of TNT-growth.

Once the TNTs are formed between adjacent B cells, naturally, the next question is how they may participate in the communication between these cells. Transfer of H-Ras signaling protein, or CD86 immune costimulator from B cell to T cell via membrane nanotubes was reported recently [33]. Here we demonstrate that MHC-II complexes or B7 family costimulatory proteins (e.g. CD86) can be found along the membrane of the nanotube and also in the membrane of the recipient cells, suggesting their exchange between B cells via membrane nanotubes. Our imaging data provide solid evidence of their presence on

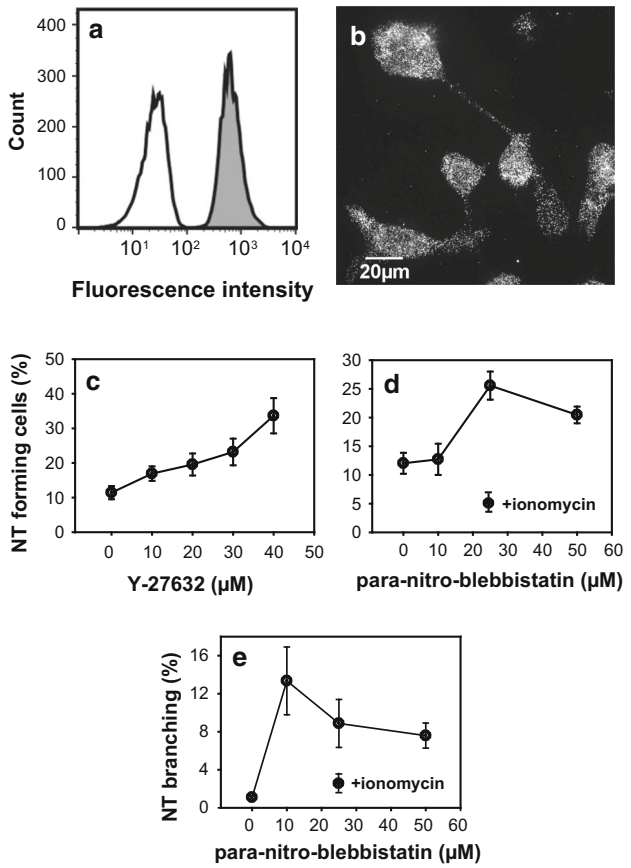

Fig. 6 Non-muscle myosin 2 also controls B cell nanotube formation. **a** Flow cytometric histograms (*white* isotype control antibody; *grey* NM2A antibody; both detected with an Alexa488-secondary antibody) show high level of NM2A in A20 B cells. **b** Representative SIM image of anti-NM2A stained A20 B cells: the motor protein localized in both the cell bodies and in the nanotubes. **c** Suppressing myosin 2 activity through Rho-kinase inhibition with Y-27632, enhanced (ca. threefold) the TNT formation in a concentration-dependent manner. **d**, **e** Para-nitro-blebbistatin, an efficient inhibitor of myosin 2 also caused a more than twofold increase in TNT number (**d**) or branching degree (**e**) in the concentration range leaving cell viability unchanged. Ionomycin (1 µg/ml) could fully impair the effect of 25 µM para-nitro-blebbistatin (**d**, **e**). (The mean ± SD data were derived from at least three independent measurements with ca. 300 cells/sample)

the other side of the connecting nanotubes. However, in this study the potential transfer was homo-cellular, such that it may significantly alter the abundance of certain MHC-II complexes or costimulatory proteins at a single-cell level. MHC-II and CD86 molecules have also been reported to be present in extracellular vesicles released by various immune cells [28, 29] and proposed to induce in this manner a positive immunregulatory role in induction of T cell-mediated immune response [28]. B cells can also function as antigen-presenting cells and thus the intercellular transport of MHC-II enriched lipid rafts [59] through nanotubes could serve to spread antigens and consequently improve the efficiency of antigen-dependent T cell activation [60].

Here we also demonstrate that B cells may also exchange intact organelles, such as lysosomes or mitochondria. Acto-myosin-dependent exchange of endocytic organelles via TNTs has been reported by Gurke et al. [61] between normal rat kidney cells. Nanotubular intercellular transfer of mitochondria was also found to rescue apoptotic PC12 cells in culture [62]. Thus, the transport of any lysosomal degradation product or a rescuing mechanism from cell death may be available for B cells through these nanotubular connections, as well. An exchange of BCR between bystander and activated B cells through spontaneous membrane transfer was also reported and speculated to be the consequence of nanotubular communication [63, 64].

Another important aim of our study was to investigate the regulation of the outgrowth-retraction equilibrium of nanotubes in B cells since the mechanistic details of nanotube dynamics in different cell types are still poorly understood. To date there are data showing that F-actin is an essential element of TNT growth in many cell types, including primary B-cell precursor leukemia cells [34]. Our data clearly demonstrate that F-actin bundles may serve as a scaffold for the growing NTs which also proved to be essential for formation of B cell nanotube networks. In accordance with findings in many other cell types, such as macrophages, T cells or kidney cells [3, 4, 6, 7, 31, 34, 65], our study also shows that inhibition of actin polymerization results in an almost complete disappearance of TNTs.

In addition to the presence of F-actin we also show that microtubules are frequent constituents of B cell nanotubes (in >85 %), similarly to earlier reports of TNTs between phagocytes or dendritic cells [2, 3, 15]. However, our results indicate that in B cells the function of microtubules are not structural but instead may be restricted to transport of various vesicles or organelles along the tubes possibly by the assistance of dynein or kinesin motor proteins, as the inhibition of their polymerization did not affect nanotube dynamics. The possibility of microtubule-assisted transport, however, awaits further exploration.

We also found that the remodeling of the cortical actin cytoskeleton in B cells was Ca^{2+}-dependent in accordance with earlier studies [1, 66], proposing that actin polymerization is important for active protrusions including TNT growth. This finding is also in accordance with earlier data showing close inverse relationship between the local cytoplasmic Ca^{2+}-level and the degree of actin polymerization/depolymerization in lymphocytes [35, 46]. Direct stimulation of the B cell receptor results in a transient rise in cytoplasmic Ca^{2+} [67, 68]. Consistent with this, our data show less TNTs in B cells stimulated via BCR. By contrast, LPS binding to B cells utilizes different receptors and

signaling pathway(s) [69] without the dominance of Ca^{2+}-dependent actin remodeling. This was in agreement with the elevated TNT frequency upon LPS-treatment, similarly to earlier data reporting increased formation of TNT-like structures in rat cornea membranes [17].

Conceivably, the dynamic assembly and disassembly of actin filaments provide essential forces for controlling the growth-retraction equilibrium of nanotubes. Further components of this actin machinery are yet to be described, but probably a set of actin-binding proteins (e.g. profilin, cofilin or gelsolin) [35, 70] similar to those involved in filopodial growth could be implicated with nanotube elongation or retraction as well.

In regards to TNTs, the regulatory effect of non-muscle myosin 2 motor proteins may be explained by assuming two antagonistic complex molecular machineries regulating the shape and locomotion of cells. Based on the direction and nature of forces, these proteins may drive a cytoskeletal network responsible for *contraction* or another one for *protrusion*. These two machineries are balanced in cells with their temporal and spatial regulation determining when and where either of these processes will occur in the cells. Induction or inhibition of the activity of these protein systems can sensitively influence the equilibrium resulting in the dominance of one of the machineries [52]. In our experiments, p-nitro-blebbistatin blocked the force generation by NM2 motors and thus inhibited the inward force on the actin filaments, while the protrusion system powered by actin polymerization was not affected. As a result, the activity of the protrusion system was more pronounced, and hence more nanotubes grew from the plasma membrane. Moreover, ROCK inhibition had a similar effect by not allowing myosin light chain phosphorylation to turn on the motor activity. Similar effects of myosin inhibition on TNT growth in Jurkat T cells [53] and normal rat kidney cells [61] also support this explanation. While all three non-muscle myosin 2 isoforms are indiscriminately inhibited by p-nitro-blebbistatin, NM2A is the major isoform found at the leading edge of polarized cells and was shown here to be present in and around B cell nanotubes. Currently, we cannot exclude that NM2A may have an effect on TNT dynamics besides driving the retrograde actin flow, for instance by regulating integrin-dependent cell adhesion [52] which is shown above to be another important factor involved in nanotube formation. However, our data clearly show that NM2A has an important negative regulatory role in nanotube generation. Although its exact mechanism is not yet known, force or tension generation by NM2 is apparently responsible for the proper maintenance of the balance between growth and retraction of nanotubular network.

Last, in previous experiments on nanotubes that were pulled out of liposomes it has been demonstrated that branching can occur when the roots of two neighboring nanotubes merge and the nanotubes coalesce [24]. Coalescence continues until the angles between the arms of the Y-shaped branching point become 120°. To note, in this study we have observed a correlation between the degree of branching and the frequency of nanotubes, which is consistent with the hypothesis that the branching of TNT-s is also the result of nanotube coalescence.

Conclusion

Here we report that murine and human B cells can spontaneously grow membrane nanotubes. Several key components and mechanisms controlling the formation-retraction equilibrium of nanotubular connections between B cells were identified. These included the interaction of cell surface integrins with extracellular matrix components, specifically $\alpha_5\beta_1$ integrins with fibronectin and $\alpha_6\beta_1$ with laminin, the subsequent cell spreading and Ca^{2+}-dependent actin remodeling. Microtubules were shown to be present in most B cell nanotubes, but in contrast to F-actin, they were not essential for their formation. Their possible functional contribution might be mediation of vesicular transport inside the nanotubes. Finally, here we provide the first evidence that non-muscle myosin 2A may act as a negative regulator of nanotube formation, but its relationship with the Ca^{2+}-dependent actin reorganization still remains unclear and requires further investigations.

As an important result, our in vitro live cell imaging data convincingly demonstrate intercellular transfer of 2–300 nm size vesicles inside the nanotubes and the possible transport of two key molecules, MHC-II and B7 costimulatory proteins involved in activation of the T-cell dependent immune defense, in the membrane of nanotubes. The transport of these molecules either in vesicles or inside the membrane of TNTs may provide a novel alternative pathway of antigen-transfer/spreading between B cells in different immune organs, such as the spleen or lymph nodes. Obviously, the important aspect of how these intercellular communication channels may form and function in vivo in the immune organs remains to be elucidated. Although results from TNT formation in 3D ECM models [3] and in vivo data [17, 18] are currently available and support their existence, verification of the many in vitro findings and models awaits further in vivo studies.

Acknowledgments This work was supported by grants T 104971 (to JM), NN 107776 and K112794 (to MN), K108437 (to LN) and K109480 (to MK) sponsored by the Hungarian National Science Fund (OTKA) and partly by MedinProt Project (Hungarian Academy of Sciences) to JM. We thank National Development Agency (NFU) and the European Social Fund for partly supporting this project by Grant Agreement TÁMOP 4.2.1./B-09/1/KMR-2010-0003. The authors are

grateful to Drs. András Málnási-Csizmadia, Boglárka Várkuti, Miklós Képíró, Mihály Kovács, Judit Ovádi, Andrea Balogh, Glória László, and Imre Derényi for valuable advice and discussions throughout this work and to Ms. Márta Pásztor and Árpád Mikesy for their skillful technical assistance. The authors are very grateful to Xabier Osteikoetxea for careful reading and for the English language revisions of the manuscript, as well as, for the valuable discussions.

References

1. Rustom A, Saffrich R, Markovic I, Walther P, Gerdes HH (2004) Nanotubular highways for intercellular organelle transport. Science 303(5660):1007–1010. doi:10.1126/science.1093133
2. Onfelt B, Nedvetzki S, Yanagi K, Davis DM (2004) Cutting edge: membrane nanotubes connect immune cells. J Immunol 173(3):1511–1513
3. Davis DM, Sowinski S (2008) Membrane nanotubes: dynamic long-distance connections between animal cells. Nat Rev Mol Cell Biol 9(6):431–436. doi:10.1038/nrm2399
4. Gurke S, Barroso JF, Gerdes HH (2008) The art of cellular communication: tunneling nanotubes bridge the divide. Histochem Cell Biol 129(5):539–550. doi:10.1007/s00418-008-0412-0
5. Gerdes HH, Carvalho RN (2008) Intercellular transfer mediated by tunneling nanotubes. Curr Opin Cell Biol 20(4):470–475. doi:10.1016/j.ceb.2008.03.005
6. Onfelt B, Nedvetzki S, Benninger RK, Purbhoo MA, Sowinski S, Hume AN, Seabra MC, Neil MA, French PM, Davis DM (2006) Structurally distinct membrane nanotubes between human macrophages support long-distance vesicular traffic or surfing of bacteria. J Immunol 177(12):8476–8483
7. Gerdes HH, Bukoreshtliev NV, Barroso JF (2007) Tunneling nanotubes: a new route for the exchange of components between animal cells. FEBS Lett 581(11):2194–2201. doi:10.1016/j.febslet.2007.03.071
8. Gousset K, Schiff E, Langevin C, Marijanovic Z, Caputo A, Browman DT, Chenouard N, de Chaumont F, Martino A, Enninga J, Olivo-Marin JC, Mannel D, Zurzolo C (2009) Prions hijack tunnelling nanotubes for intercellular spread. Nat Cell Biol 11(3):328–336. doi:10.1038/ncb1841
9. Smith IF, Shuai J, Parker I (2011) Active generation and propagation of Ca^{2+} signals within tunneling membrane nanotubes. Biophys J 100(8):L37–L39. doi:10.1016/j.bpj.2011.03.007
10. He K, Luo W, Zhang Y, Liu F, Liu D, Xu L, Qin L, Xiong C, Lu Z, Fang X (2010) Intercellular transportation of quantum dots mediated by membrane nanotubes. ACS Nano 4(6):3015–3022. doi:10.1021/nn1002198
11. Wang X, Bukoreshtliev NV, Gerdes HH (2012) Developing neurons form transient nanotubes facilitating electrical coupling and calcium signaling with distant astrocytes. PLoS One 7(10):e47429. doi:10.1371/journal.pone.0047429
12. Wang X (1818) Gerdes HH (2012) Long-distance electrical coupling via tunneling nanotubes. Biochim Biophys Acta 8:2082–2086. doi:10.1016/j.bbamem.2011.09.002
13. Wang X, Veruki ML, Bukoreshtliev NV, Hartveit E, Gerdes HH (2010) Animal cells connected by nanotubes can be electrically coupled through interposed gap-junction channels. Proc Natl Acad Sci USA 107(40):17194–17199. doi:10.1073/pnas.1006785107
14. Ranzinger J, Rustom A, Abel M, Leyh J, Kihm L, Witkowski M, Scheurich P, Zeier M, Schwenger V (2011) Nanotube action between human mesothelial cells reveals novel aspects of inflammatory responses. PLoS One 6(12):e29537. doi:10.1371/journal.pone.0029537
15. Austefjord MW, Gerdes HH, Wang X (2014) Tunneling nanotubes: diversity in morphology and structure. Commun Integr Biol 7(1):e27934. doi:10.4161/cib.27934
16. Van den Broeke C, Radu M, Deruelle M, Nauwynck H, Hofmann C, Jaffer ZM, Chernoff J, Favoreel HW (2009) Alphaherpesvirus US3-mediated reorganization of the actin cytoskeleton is mediated by group A p21-activated kinases. Proc Natl Acad Sci USA 106(21):8707–8712. doi:10.1073/pnas.0900436106
17. Chinnery HR, Pearlman E, McMenamin PG (2008) Cutting edge: membrane nanotubes in vivo: a feature of MHC class II + cells in the mouse cornea. J Immunol 180(9):5779–5783
18. Seyed-Razavi Y, Hickey MJ, Kuffova L, McMenamin PG, Chinnery HR (2013) Membrane nanotubes in myeloid cells in the adult mouse cornea represent a novel mode of immune cell interaction. Immunol Cell Biol 91(1):89–95. doi:10.1038/icb.2012.52
19. Teddy JM, Kulesa PM (2004) In vivo evidence for short- and long-range cell communication in cranial neural crest cells. Development 131(24):6141–6151. doi:10.1242/dev.01534
20. Caneparo L, Pantazis P, Dempsey W, Fraser SE (2011) Intercellular bridges in vertebrate gastrulation. PLoS One 6(5):e20230. doi:10.1371/journal.pone.0020230
21. Pyrgaki C, Trainor P, Hadjantonakis AK, Niswander L (2010) Dynamic imaging of mammalian neural tube closure. Dev Biol 344(2):941–947. doi:10.1016/j.ydbio.2010.06.010
22. Derenyi I, Julicher F, Prost J (2002) Formation and interaction of membrane tubes. Phys Rev Lett 88(23):238101
23. Derényi I et al (2007) Membrane Nanotubes. Lecture Notes Physics, 711. In: Controlled Nanoscale Motion: Nobel Symposium, vol. 131, pp 141–159
24. Cuvelier D, Derenyi I, Bassereau P, Nassoy P (2005) Coalescence of membrane tethers: experiments, theory, and applications. Biophys J 88(4):2714–2726. doi:10.1529/biophysj.104.056473
25. Roux A, Cuvelier D, Nassoy P, Prost J, Bassereau P, Goud B (2005) Role of curvature and phase transition in lipid sorting and fission of membrane tubules. EMBO J 24(8):1537–1545. doi:10.1038/sj.emboj.7600631
26. Veranic P, Lokar M, Schutz GJ, Weghuber J, Wieser S, Hagerstrand H, Kralj-Iglic V, Iglic A (2008) Different types of cell-to-cell connections mediated by nanotubular structures. Biophys J 95(9):4416–4425. doi:10.1529/biophysj.108.131375
27. Lokar M, Kabaso D, Resnik N, Sepcic K, Kralj-Iglic V, Veranic P, Zorec R, Iglic A (2012) The role of cholesterol-sphingomyelin membrane nanodomains in the stability of intercellular membrane nanotubes. Int J Nanomed 7:1891–1902. doi:10.2147/IJN.S28723
28. Thery C, Ostrowski M, Segura E (2009) Membrane vesicles as conveyors of immune responses. Nat Rev Immunol 9(8):581–593. doi:10.1038/nri2567
29. Gyorgy B, Szabo TG, Pasztoi M, Pal Z, Misjak P, Aradi B, Laszlo V, Pallinger E, Pap E, Kittel A, Nagy G, Falus A, Buzas EI (2011) Membrane vesicles, current state-of-the-art: emerging role of extracellular vesicles. Cell Mol Life Sci CMLS 68(16):2667–2688. doi:10.1007/s00018-011-0689-3
30. Osteikoetxea X, Nemeth A, Sodar BW, Vukman KV, Buzas EI (2016) Extracellular vesicles in cardiovascular diseases, are they Jedi or Sith? J Physiol. doi:10.1113/JP271336
31. Davis DM (2009) Mechanisms and functions for the duration of intercellular contacts made by lymphocytes. Nat Rev Immunol 9(8):543–555. doi:10.1038/nri2602
32. Marzo L, Gousset K, Zurzolo C (2012) Multifaceted roles of tunneling nanotubes in intercellular communication. Front Physiol 3:72. doi:10.3389/fphys.2012.00072

33. Rainy N, Chetrit D, Rouger V, Vernitsky H, Rechavi O, Marguet D, Goldstein I, Ehrlich M, Kloog Y (2013) H-Ras transfers from B to T cells via tunneling nanotubes. Cell Death Dis 4:e726. doi:10.1038/cddis.2013.245
34. Polak R, de Rooij B, Pieters R, den Boer ML (2015) B-cell precursor acute lymphoblastic leukemia cells use tunneling nanotubes to orchestrate their microenvironment. Blood 126(21):2404–2414. doi:10.1182/blood-2015-03-634238
35. Maus M, Medgyesi D, Kiss E, Schneider AE, Enyedi A, Szilagyi N, Matko J, Sarmay G (2013) B cell receptor-induced Ca^{2+} mobilization mediates F-actin rearrangements and is indispensable for adhesion and spreading of B lymphocytes. J Leukoc Biol 93(4):537–547. doi:10.1189/jlb.0312169
36. Maloney DG, Kaminski MS, Burowski D, Haimovich J, Levy R (1985) Monoclonal anti-idiotype antibodies against the murine B cell lymphoma 38C13: characterization and use as probes for the biology of the tumor in vivo and in vitro. Hybridoma 4(3):191–209
37. Hathcock KS, Laszlo G, Dickler HB, Bradshaw J, Linsley P, Hodes RJ (1993) Identification of an alternative CTLA-4 ligand costimulatory for T cell activation. Science 262(5135):905–907
38. Gungor B, Gombos I, Crul T, Ayaydin F, Szabo L, Torok Z, Mates L, Vigh L, Horvath I (2014) Rac1 participates in thermally induced alterations of the cytoskeleton, cell morphology and lipid rafts, and regulates the expression of heat shock proteins in B16F10 melanoma cells. PLoS One 9(2):e89136. doi:10.1371/journal.pone.0089136
39. Kellermayer MS, Karsai A, Kengyel A, Nagy A, Bianco P, Huber T, Kulcsar A, Niedetzky C, Proksch R, Grama L (2006) Spatially and temporally synchronized atomic force and total internal reflection fluorescence microscopy for imaging and manipulating cells and biomolecules. Biophys J 91(7):2665–2677. doi:10.1529/biophysj.106.085456
40. Sowinski S, Jolly C, Berninghausen O, Purbhoo MA, Chauveau A, Kohler K, Oddos S, Eissmann P, Brodsky FM, Hopkins C, Onfelt B, Sattentau Q, Davis DM (2008) Membrane nanotubes physically connect T cells over long distances presenting a novel route for HIV-1 transmission. Nat Cell Biol 10(2):211–219. doi:10.1038/ncb1682
41. Puklin-Faucher E, Gao M, Schulten K, Vogel V (2006) How the headpiece hinge angle is opened: new insights into the dynamics of integrin activation. J Cell Biol 175(2):349–360. doi:10.1083/jcb.200602071
42. Ambrose HE, Wagner SD (2004) α6-Integrin is expressed on germinal center B cells and modifies growth of a B-cell line. Immunology 111:400–406. doi:10.1111/j.1365-2567.2004.01824.x
43. Chen L, Vicente-Manzanares M, Potvin-Trottier L, Wiseman PW, Horwitz AR (2012) The integrin-ligand interaction regulates adhesion and migration through a molecular clutch. PLoS One 7(7):e40202. doi:10.1371/journal.pone.0040202
44. Danen EH, Sonneveld P, Brakebusch C, Fassler R, Sonnenberg A (2002) The fibronectin-binding integrins alpha5beta1 and alphavbeta3 differentially modulate RhoA-GTP loading, organization of cell matrix adhesions, and fibronectin fibrillogenesis. J Cell Biol 159(6):1071–1086. doi:10.1083/jcb.200205014
45. Osteikoetxea X, Balogh A, Szabo-Taylor K, Nemeth A, Szabo TG, Paloczi K, Sodar B, Kittel A, Gyorgy B, Pallinger E, Matko J, Buzas EI (2015) Improved characterization of EV preparations based on protein to lipid ratio and lipid properties. PLoS One 10(3):e0121184. doi:10.1371/journal.pone.0121184
46. Babich A, Burkhardt JK (2013) Coordinate control of cytoskeletal remodeling and calcium mobilization during T-cell activation. Immunol Rev 256(1):80–94. doi:10.1111/imr.12123
47. Sayyad WA, Amin L, Fabris P, Ercolini E, Torre V (2015) The role of myosin-II in force generation of DRG filopodia and lamellipodia. Sci Rep 5:7842. doi:10.1038/srep07842
48. Ilani T, Vasiliver-Shamis G, Vardhana S, Bretscher A, Dustin ML (2009) T cell antigen receptor signaling and immunological synapse stability require myosin IIA. Nat Immunol 10(5):531–539. doi:10.1038/ni.1723
49. Kumari S, Vardhana S, Cammer M, Curado S, Santos L, Sheetz MP, Dustin ML (2012) T lymphocyte myosin IIA is required for maturation of the immunological synapse. Front Immunol 3:230. doi:10.3389/fimmu.2012.00230
50. Manes TD, Pober JS (2013) TCR-driven transendothelial migration of human effector memory CD4 T cells involves Vav, Rac, and myosin IIA. J Immunol 190(7):3079–3088. doi:10.4049/jimmunol.1201817
51. Kepiro M, Varkuti BH, Vegner L, Voros G, Hegyi G, Varga M, Malnasi-Csizmadia A (2014) Para-nitroblebbistatin, the non-cytotoxic and photostable myosin II inhibitor. Angew Chem Int Ed Engl 53(31):8211–8215. doi:10.1002/anie.201403540
52. Vicente-Manzanares M, Ma X, Adelstein RS, Horwitz AR (2009) Non-muscle myosin II takes centre stage in cell adhesion and migration. Nat Rev Mol Cell Biol 10(11):778–790. doi:10.1038/nrm2786
53. Obermajer N, Jevnikar Z, Doljak B, Sadaghiani AM, Bogyo M, Kos J (2009) Cathepsin X-mediated beta2 integrin activation results in nanotube outgrowth. Cell Mol Life Sci CMLS 66(6):1126–1134. doi:10.1007/s00018-009-8829-8
54. Sa S, Wong L, McCloskey KE (2014) Combinatorial fibronectin and laminin signaling promote hoghly efficient cardiac differentiation of human embryonic stem cells. Biores Open Access 3(4):150–161. doi:10.1089/biores.2014.0018
55. Ramos Gde O, Bernardi L, Lauxen I, Sant'Ana Filho M, Horwitz AR, Lamers ML (2016) Fibronectin modulates cell adhesion and signaling to promote single cell migration of highly invasive oral squamous cell carcinoma. PLoS One 11(3):e0151338. doi:10.1371/journal.pone.0151338
56. Yarwood SJ, Woodgett JR (2001) Extracellular matrix composition determines the transcriptional response to epidermal growth factor receptor activation. Proc Natl Acad Sci USA 98:4472–4477. doi:10.1073/pnas.081069098
57. Borland G, Cushley W (2004) Positioning the immune system: unexpected roles for α6-integrins. Immunology 111:381–383. doi:10.1111/j.1365-2567.2004.01838.x
58. Thayanithy V, Babatunde V, Dickson EL, Wong P, Oh S, Ke X, Barlas A, Fujisawa S, Romin Y, Moreira AL, Downey RJ, Steer CJ, Subramanian S, Manova-Todorova K, Moore MA, Lou E (2014) Tumor exosomes induce tunneling nanotubes in lipid raft-enriched regions of human mesothelioma cells. Exp Cell Res 323(1):178–188. doi:10.1016/j.yexcr.2014.01.014
59. Gombos I, Detre C, Vamosi G, Matko J (2004) Rafting MHC-II domains in the APC (presynaptic) plasma membrane and the thresholds for T-cell activation and immunological synapse formation. Immunol Lett 92(1–2):117–124. doi:10.1016/j.imlet.2003.11.022
60. Anderson HA, Hiltbold EM, Roche PA (2000) Concentration of MHC class II molecules in lipid rafts facilitates antigen presentation. Nat Immunol 1(2):156–162. doi:10.1038/77842
61. Gurke S, Barroso JF, Hodneland E, Bukoreshtliev NV, Schlicker O, Gerdes HH (2008) Tunneling nanotube (TNT)-like structures facilitate a constitutive, actomyosin-dependent exchange of endocytic organelles between normal rat kidney cells. Exp Cell Res 314(20):3669–3683. doi:10.1016/j.yexcr.2008.08.022
62. Wang X, Gerdes HH (2015) Transfer of mitochondria via tunneling nanotubes rescues apoptotic PC12 cells. Cell Death Differ 22(7):1181–1191. doi:10.1038/cdd.2014.211
63. Poupot M, Fournie JJ (2003) Spontaneous membrane transfer through homotypic synapses between lymphoma cells. J Immunol 171(5):2517–2523

64. Quah BJ, Barlow VP, McPhun V, Matthaei KI, Hulett MD, Parish CR (2008) Bystander B cells rapidly acquire antigen receptors from activated B cells by membrane transfer. Proc Natl Acad Sci USA 105(11):4259–4264. doi:10.1073/pnas.0800259105
65. Bukoreshtliev NV, Wang X, Hodneland E, Gurke S, Barroso JF, Gerdes HH (2009) Selective block of tunneling nanotube (TNT) formation inhibits intercellular organelle transfer between PC12 cells. FEBS Lett 583(9):1481–1488. doi:10.1016/j.febslet.2009.03.065
66. Zhu D, Tan KS, Zhang X, Sun AY, Sun GY, Lee JC (2005) Hydrogen peroxide alters membrane and cytoskeleton properties and increases intercellular connections in astrocytes. J Cell Sci 118(Pt 16):3695–3703. doi:10.1242/jcs.02507
67. Kiss E, Sarmay G, Matko J (2006) Ceramide modulation of antigen- triggered Ca2 + signals and cell fate: diversity in the responses of various immunocytes. Ann N Y Acad Sci 1090:161–167. doi:10.1196/annals.1378.017
68. Monroe JG, Cambier JC (1983) B cell activation. III. B cell plasma membrane depolarization and hyper-Ia antigen expression induced by receptor immunoglobulin cross-linking are coupled. J Exp Med 158(5):1589–1599
69. Brown J, Wang H, Hajishengallis GN, Martin M (2011) TLR-signaling networks: an integration of adaptor molecules, kinases, and cross-talk. J Dent Res 90(4):417–427. doi:10.1177/0022034510381264
70. Samstag Y, Eibert SM, Klemke M, Wabnitz GH (2003) Actin cytoskeletal dynamics in T lymphocyte activation and migration. J Leukoc Biol 73(1):30–48